Temperature explains broad patterns of Ross River virus transmission across Australia

Marta S. Shocket[1*] (mshocket@stanford.edu), Sadie J. Ryan[2,3,4] (sjryan@ufl.edu), and Erin A. Mordecai[1] (emordeca@stanford.edu)

[1]Department of Biology, Stanford University, 371 Serra Mall, Stanford, CA, USA

[2]Department of Geography, University of Florida, Turlington Hall, Gainesville, FL, USA

[3]Emerging Pathogens Institute, University of Florida, Gainesville, FL, USA

[4]School of Life Sciences, College of Agriculture, Engineering, and Science, University of KwaZulu Natal, Scottsville, KwaZulu Natal, South Africa

Statement of authorship: EAM conceived of and designed the study. MSS collected data, performed statistical analyses, and wrote the first draft of the manuscript. SJR performed geographic analyses. All authors revised the manuscript.

Data accessibility statement: Upon acceptance, all data will be archived in a public repository.

Keywords: *Aedes vigilax*, arbovirus, *Culex annulirostris*, mosquito-borne disease, infectious disease, Murray Valley Encephalitis virus, Ross River virus, R0 model, temperature, vector-borne disease

Running Title: Temperature & Ross River virus transmission **Article type**: Letter

Words in abstract: 147 **Words in main text**: 5000 **Number of references**: 94

Number of figures, tables and text boxes: 6 figures, no tables or text boxes

* Corresponding Author: Marta S. Shocket, mshocket@stanford.edu, phone: 650-723-5923

ABSTRACT

Temperature impacts the physiology of ectotherms, including vectors that transmit disease. While thermal biology predicts nonlinear effects of temperature on vector and pathogen traits that drive disease transmission, the empirical relationship between temperature and transmission remains unknown for most vector-borne pathogens. We built a mechanistic model to estimate the thermal response of Ross River virus, an important mosquito-borne pathogen of humans in Australia, the Pacific Islands, and potentially emerging worldwide. Transmission peaks at moderate temperatures (26.4°C) and declines to zero at low (17.0°C) and high (31.5°C) temperatures. The model predicted broad patterns of disease across Australia. First, transmission is year-round endemic in the tropics and sub-tropics but seasonal in temperate zones. Second, nationwide human cases peak seasonally as predicted from population-weighted seasonal temperatures. These results illustrate the importance of nonlinear, mechanistic models for inferring the role of temperature in disease dynamics and predicting responses to climate change.

38 **INTRODUCTION**

39 Temperature impacts mosquito-borne disease transmission via effects on the physiology
40 of mosquitoes and pathogens (Shocket *et al.* n.d.). Transmission requires that mosquitoes be
41 abundant, bite a host and ingest an infectious bloodmeal, survive long enough for pathogen
42 development and within-host migration (the extrinsic incubation period), and bite additional
43 hosts (Shocket *et al.* n.d.). All of these processes depend on temperature. Support for temperature
44 effects on mosquito-borne disease arises from mechanistic models based on thermal biology
45 (Mordecai *et al.* 2013, 2017; Liu-Helmersson *et al.* 2014; Wesolowski *et al.* 2015; Paull *et al.*
46 2017) and statistical models that analyze variation in climate and disease over time and space
47 (Werner *et al.* 2012; Stewart Ibarra & Lowe 2013; Siraj *et al.* 2015; Paull *et al.* 2017). However,
48 important knowledge gaps remain. First, variation in how transmission responds to temperature
49 across mosquito-borne diseases, and via what mechanisms, remains uncertain. Accordingly, the
50 types of data needed to characterize thermal responses of additional or emerging diseases are
51 unclear. Second, the impacts of temperature on transmission can appear idiosyncratic across
52 locations and studies (Hu *et al.* 2004; Gatton *et al.* 2005; Jacups *et al.* 2008a; Bi *et al.* 2009;
53 Werner *et al.* 2012; Koolhof *et al.* 2017), and inferring causality from field observations and
54 statistical approaches alone remains challenging. Thermal biology may provide an explanation
55 for this variation or a causal link. Filling these gaps is necessary to predict geographic, seasonal,
56 and interannual variation in transmission of mosquito-borne pathogens, especially as the climate
57 changes. Here, we address these gaps by building a model for temperature-dependent
58 transmission of Ross River virus.

59 Ross River virus (RRV) is a mosquito-transmitted alphavirus that causes the most
60 common mosquito-borne disease in Australia (1,500–9,500 human cases per year; Koolhof &

61 Carver 2017). RRV is also endemic in Pacific Island nations, following a 1979-80 epidemic that
62 infected over 500,000 people (Klapsing *et al.* 2005; Aubry *et al.* 2015; Lau *et al.* 2017). RRV
63 infection causes acute fever, rash, and joint pain, which can become chronic and cause disability
64 (Harley *et al.* 2001). In some cases temperature predicts RRV cases (Gatton *et al.* 2005; Bi *et al.*
65 2009; Werner *et al.* 2012), while other cases it does not (Hu *et al.* 2004; Gatton *et al.* 2005).
66 Understanding RRV transmission ecology is critical because the virus is a likely candidate for
67 emergence worldwide (Flies *et al.* 2018). A mechanistic model for temperature-dependent RRV
68 transmission could help explain these disparate results and predict potential expansion.
69 Mechanistic models synthesize how environmental factors like temperature influence the
70 host and parasite traits that drive transmission. For ectotherms, these traits depend nonlinearly on
71 environmental temperature. Specifically, trait thermal responses are usually unimodal: they peak
72 at an intermediate temperature optimum and decline towards zero at lower and upper thermal
73 limits, all of which can vary across traits (Angilletta 2009; Dell *et al.* 2011; Mordecai *et al.* 2013,
74 2017). Mechanistic models combine the multiple, nonlinear thermal responses that shape
75 transmission (Rogers & Randolph 2006; Mordecai *et al.* 2013). One commonly-used measure of
76 disease spread is R_0, the basic reproductive number (expected number of secondary cases from a
77 single case in a fully susceptible population). For mosquito-borne disease, R_0 is a nonlinear
78 function of mosquito density, biting rate, vector competence (infectiousness given pathogen
79 exposure), and adult survival; pathogen extrinsic incubation period; and human recovery rate
80 (Dietz 1993). To understand the overall impact of temperature on transmission, we can
81 incorporate empirically-estimated trait thermal responses into an R_0 model. Incorporating the full
82 suite of nonlinear trait responses often produces predictions that are drastically different than
83 models that assume linear or monotonic thermal responses or omit important temperature-

84 dependent processes (Mordecai *et al.* 2013, 2017). Previous mechanistic models have predicted
85 different optimal temperatures for disease spread across pathogens and vector species: 25 ºC for
86 *falciparum* malaria and West Nile virus (Mordecai *et al.* 2013; Paull *et al.* 2017), and 29ºC and
87 26 ºC for dengue, chikungunya, and Zika viruses in *Ae. aegypti* and in *Ae. albopictus*,
88 respectively (Liu-Helmersson *et al.* 2014; Wesolowski *et al.* 2015; Mordecai *et al.* 2017).
89 In this paper, we build the first mechanistic model for temperature-dependent
90 transmission of RRV and ask whether temperature explains seasonal and geographic patterns of
91 disease spread. We use data from laboratory experiments with the two most important and well-
92 studied vector species (*Culex annulirostris* and *Aedes vigilax*) to parameterize the model with
93 unimodal thermal responses. We then use sensitivity and uncertainty analyses to determine
94 which traits drive the relationship between temperature and transmission potential and identify
95 key data gaps. Finally, we illustrate how temperature currently shapes patterns of disease across
96 Australia. The model correctly predicts that RRV disease should be year-round endemic in
97 tropical, northern Australia and seasonally epidemic in temperate, southern Australia. It also
98 accurately predicts the seasonality of human cases nationally. Thus, the temperature-dependent
99 model for RRV transmission provides a mechanistic link between geographic and seasonal
100 changes in temperature and broad-scale patterns of disease.
101
102 **MATERIAL AND METHODS**
103 *Natural History of RRV*
104 The natural history of RRV is complex: transmission occurs across a range of climates
105 (tropical, subtropical, and temperate) and habitats (urban and rural, coastal and inland) and via
106 many vector and vertebrate reservoir species (Claflin & Webb 2015; Stephenson *et al.* 2018).

107 The virus has been isolated from over 40 mosquito species in nature, and 10 species transmit it in
108 laboratory studies (Harley *et al.* 2001; Russell 2002). However, four key species are responsible
109 for most transmission to humans (*Culex annulirostris*, *Aedes [Ochlerotatus] vigilax*, *Ae. [O.]*
110 *notoscriptus*, and *Ae. [O.] camptorhynchus*), with two additional species also implicated in
111 human outbreaks (*Ae. [Stegomyia] polynesiensis* and *Ae. [O.] normanensis*).
112 The vectors differ in climate and habitat niches, leading to geographic variation in
113 associations with outbreaks. We assembled and mapped records of RRV outbreaks in humans
114 attributed to specific species (Fig. 1, Table S1 in Appendix S1 in Supporting Information; Rosen
115 *et al.* 1981; Campbell *et al.* 1989; Russell *et al.* 1991; Lindsay *et al.* 1992, 1993a, b, 1996, 2007;
116 McManus *et al.* 1992; Merianos *et al.* 1992; Whelan *et al.* 1992, 1995, 1997; McDonnell *et al.*
117 1994; Russell 1994, 2002; Dhileepan 1996; Ritchie *et al.* 1997; Brokenshire *et al.* 2000; Ryan *et*
118 *al.* 2000; Harley *et al.* 2000, 2001; Frances *et al.* 2004; Kelly-Hope *et al.* 2004b; Biggs &
119 Mottram 2008; Schmaedick *et al.* 2008; Jacups *et al.* 2008b; Lau *et al.* 2017). *Ae. vigilax* and *Ae.*
120 *notoscriptus* contribute to transmission more in tropical and subtropical zones, *Ae.*
121 *camptorhynchus* in temperate zones, and *Cx. annulirostris* throughout all climatic zones.
122 Freshwater-breeding *Cx. annulirostris* contributes to transmission in both inland and coastal
123 areas, while saltmarsh mosquitoes *Ae. vigilax* and *Ae. camptorhynchus* contribute in coastal areas
124 (Russell 2002) and inland areas affected by salinization from agriculture (Biggs & Mottram
125 2008; Carver *et al.* 2009). Peri-domestic, container-breeding *Ae. notoscriptus* contributes in
126 urban areas (Russell 2002; Faull & Williams 2016). The vectors also differ in seasonality: *Ae.*
127 *camptorhynchus* populations peak earlier and in cooler temperatures than *Ae. vigilax*, leading to
128 seasonal succession where they overlap (Lindsay *et al.* 1992; Russell 1998). This latitudinal and

129 temporal variation suggests that vector species may have different thermal optima and/or niche
130 breadths. If so, temperature may impact disease transmission differently for each species.
131
132 *Temperature-Dependent R_0 Models*
133 R_0 depends on a suite of vector, pathogen, and human traits, including vector density.
134 Vector density in turn depends on reproduction, development rate, and survival at egg, larval,
135 pupal, and adult stages, all of which are sensitive to temperature. However, mosquito density
136 also depends on aquatic breeding habitat and other factors (Barton *et al.* 2004; Kokkinn *et al.*
137 2009; Jacups *et al.* 2015). For this reason, we developed two models of R_0: (eq. 1) the 'Constant
138 *M* Model' assumes that mosquito density (*M*) does not depend on temperature (equation from
139 Dietz 1993); (eq. 2) the 'Temperature-Dependent *M* Model' assumes that temperature drives
140 mosquito density and includes vector life history trait thermal responses (Parham & Michael
141 2010; Mordecai *et al.* 2013, 2017; Johnson *et al.* 2015). The relative influence of temperature
142 versus habitat availability and other drivers varies across settings, and these models capture two
143 extremes. Because habitat availability is context-dependent and species-specific, and because we
144 focus on temperature, we do not model vector habitat here.

145 Constant *M* Model: $$R_0(T) = \left(\frac{a(T)^2 bc(T) e^{-\frac{\mu(T)}{PDR(T)}} M}{N\, r\, \mu(T)}\right)^{1/2} \quad \text{eq. 1}$$

146 Temperature-dependent *M* Model: $$R_0(T) = \left(\frac{a(T)^2 bc(T) e^{-\frac{\mu(T)}{PDR(T)}} EFD(T) p_{EA} MDR(T)}{N\, r\, \mu(T)^3}\right)^{1/2} \quad \text{eq. 2}$$

147 In both equations, (*T*) indicates a parameter depends on temperature, *a* is mosquito biting
148 rate, *bc* is vector competence (proportion of mosquitoes that become infectious given exposure),
149 μ is adult mosquito mortality rate (adult lifespan, $lf = 1/\mu$), *PDR* is parasite development rate

150 ($PDR = 1/EIP$, the extrinsic incubation period), N is human density, and r is the rate at which
151 humans recover from infection and become immune (all rates are measured in days^{-1}). The latter
152 two terms do not depend on temperature. In the temperature-dependent M model, mosquito
153 density (M) depends on fecundity (EFD, eggs per female per day), proportion surviving from
154 egg-to-adult (p_{EA}), and mosquito development rate (MDR), divided by the square of adult
155 mortality rate (μ; Parham & Michael 2010). We calculated p_{EA} as the product of the proportion
156 of egg rafts that hatch (pRH), the number of larvae per raft that hatch (nLR, scaled by the
157 maximum at any temperature to calculate proportional egg survival within-rafts), and the
158 proportion of larvae surviving to adulthood (p_{LA}). We initially compare results for both models,
159 then focus on the temperature-dependent M model.

160 Since R_0 also depends on other factors, we scaled the model output between zero and one
161 ('relative R_0'). Relative R_0 describes the temperature suitability for transmission, which combines
162 with other factors like breeding habitat availability, vector control, humidity, human and
163 reservoir host density, host immune status, and mosquito exposure to determine disease
164 incidence. In this approach, only the relative response of each trait to temperature matters, which
165 is desirable since traits can differ substantially based on other factors and in the laboratory versus
166 the field (particularly mosquito survival: MacDonald 1952; Clements & Paterson 1981). With
167 relative R_0 we cannot use the typical threshold for sustained disease transmission ($R_0>1$).
168 However, relative R_0 preserves the temperature-dependence of R_0, including key temperature
169 values where transmission is possible ($R_0>0$; a conservative threshold where transmission is not
170 excluded by temperature) and where R_0 is maximized.

171 We fit functions describing the thermal response of each trait in the R_0 models using
172 previously published data (Table S2; (McDonald *et al.* 1980; Mottram *et al.* 1986; Russell 1986;

173 Rae 1990; Kay & Jennings 2002). We exhaustively searched the literature for laboratory studies
174 with trait measurements at three or more constant temperatures for the major vector species in
175 Australia (*Cx. annulirostris*, *Ae. vigilax*, *Ae. camptorhynchus*, *Ae. notoscriptus*, and *Ae.*
176 *normanensis*). Data were sparse: no species had data for all traits needed to parameterize the R_0
177 models (Fig. 1). Therefore, we combined mosquito life history traits from *Cx. annulirostris* (a, μ,
178 *EFD*, *pRH*, *nLR*, p_{LA}, *MDR*) and pathogen infection traits measured in *Ae. vigilax* (*bc*, *PDR*) to
179 build composite R_0 models. We also fit traits for other mosquito and virus species: *MDR* and
180 *pEA* from *Ae. camptorhynchus* and *Ae. notoscriptus*, and *PDR* and *bc* from Murray Valley
181 encephalitis virus in *Cx. annulirostris* (Appendix S1). We use sensitivity analyses to evaluate the
182 potential impact of this vector species mismatch.

183 We fit unimodal thermal responses for traits using Bayesian inference with the 'r2jags'
184 package (Plummer 2003; Su & Yajima 2009) in R (R Core Team 2017). Traits with
185 asymmetrical thermal responses were fit as Brière functions of temperature: $qT(T - T_0)(T_{max} -$
186 $T)^{1/2}$ (Brière *et al.* 1999). Traits with symmetrical thermal responses were fit as quadratic
187 functions of temperature: $-q(T - T_0)(T - T_{max})$. In both functions of temperature (T), T_0 and T_m are
188 the critical thermal minimum and maximum, respectively, and q is a rate parameter. For priors
189 we used gamma distributions where the hyperparameters were derived from thermal responses fit
190 to data from other mosquito species with similar ecology (*Ae. aegypti*, *Ae. albopictus*, *Ae.*
191 *krombeini*, and *Ae. triseriatus*, and *Anopheles pseudopunctipennis*; Table S4), allowing us to
192 more accurately represent their fit and uncertainty. Our data did not include declining trait values
193 at high temperatures for biting rate (a) and parasite development rate (*PDR*). Nonetheless, data
194 from other mosquito species (Mordecai *et al.* 2013, 2017) and principles of thermal biology
195 (Angilletta 2009; Dell *et al.* 2011) imply that these traits must decline at very high temperatures.

196 Thus, for those traits we included an artificial data point where the trait value approached zero at
197 a very high temperature (40ºC), allowing us to fit the Brière function. We used strongly
198 informative priors to limit the effect of these traits on the upper thermal limit of R_0 (by
199 constraining them to decline near 40ºC). For comparison, we also fit all thermal responses with
200 uniform priors; these results illustrate how our choices of priors impacted the results (Appendix
201 S1).
202
203 *Sensitivity and uncertainty analyses*
204 We conducted sensitivity and uncertainty analyses of the temperature-dependent M
205 model (eq. 2) to understand how trait thermal responses shape the thermal response of R_0. We
206 examined the sensitivity of R_0 in two ways. First, we evaluated the impact of each trait by setting
207 it constant while allowing all other traits to vary with temperature. Second, we calculated the
208 partial derivative of R_0 with respect to each trait across temperature (i.e., $\partial R_0/\partial X \cdot \partial X/\partial T$ for trait
209 X and temperature T; Appendix S1). We also calculated the effect of each trait on uncertainty in
210 $R_0(T)$—the proportion of total uncertainty due to each trait across temperature—to understand
211 what data would most improve the model. To do so, we first propagated posterior samples from
212 all trait thermal response distributions through to $R_0(T)$ and calculated the width of the 95%
213 highest posterior density interval (HPD interval; a type of credible interval) of this distribution at
214 each temperature: the 'full $R_0(T)$ uncertainty'. Next, we sampled each trait from its posterior
215 distribution while setting all other trait thermal responses to their posterior medians, and
216 calculated the posterior distribution of $R_0(T)$ and the width of its 95% HPD interval across
217 temperature: the 'single-trait $R_0(T)$ uncertainty'. Finally, we divided each single-trait $R_0(T)$
218 uncertainty by the full $R_0(T)$ uncertainty.

219

220 *Field Observations: Seasonality of Temperature-Dependent R_0 Across Australia*

221 We used the temperature-dependent M model (eq. 2) to predict the seasonality of $R_0(T)$
222 across Australia. We took monthly mean temperatures from WorldClim for seven cities spanning
223 a latitudinal and temperature gradient (from tropical North to temperate South: Darwin, Cairns,
224 Brisbane, Perth, Sydney, Melbourne, and Hobart) and calculated the posterior median $R_0(T)$ for
225 each month at each location. We also compared the seasonality of a population-weighted $R_0(T)$
226 with the seasonality of nationally aggregated RRV cases. We used 2016 census estimates for the
227 fifteen most populous urban areas, which together contain 76.6% of Australia's population
228 (Australian Bureau of Statistics 2017). We calculated relative $R_0(T)$ for each location and
229 weighted by population to estimate a country-wide average. We compared this country-scale
230 estimate of relative $R_0(T)$ with data on mean monthly human cases of RRV nationwide from
231 1992-2013 obtained from the National Notifiable Diseases Surveillance System.

232 We expected a substantial time lag between temperature suitability and reported human
233 cases as mosquito populations increase, bite humans and reservoir hosts, acquire RRV, become
234 infectious, and bite subsequent hosts, which then undergo an incubation period before
235 (potentially) becoming symptomatic, seeking treatment, and reporting cases. Empirical work on
236 dengue vectors in Ecuador identified a six-week time lag between temperature and mosquito
237 oviposition (Stewart Ibarra *et al.* 2013). Subsequent mosquito development and virus incubation
238 periods in mosquitoes and humans likely add another two- to four-week lag before symptomatic
239 cases appear, resulting in an 8-10 week lag between temperature and observed cases (Hu *et al.*
240 2006; Jacups *et al.* 2008b; Mordecai *et al.* 2017). With monthly case data, we hypothesize a two-
241 month time lag between $R_0(T)$ and RRV disease cases.

242

243 *Mapping Temperature-Dependent R_0 Across Australia*

244 To illustrate temperature suitability for RRV transmission across Australia, we mapped
245 the number of months for which relative $R_0(T)>0$ and >0.5 for the posterior median, 2.5%, and
246 97.5% credibility bounds (Fig. S7) based on the temperature-dependent *M* model (eq. 2). We
247 calculated relative $R_0(T)$ at 0.2°C increments and projected it onto the landscape for monthly
248 mean temperatures from WorldClim data at a 5-minute resolution (approximately 10km^2 at the
249 equator). Climate data layers were extracted for the geographic area, defined using the Global
250 Administrative Boundaries Databases (GADM 2012). We performed all map calculations and
251 manipulations in R using packages 'raster' (Hijmans 2016), 'maptools' (Bivand & Lewin-Koh
252 2017), and 'Rgdal' (Bivand *et al.* 2017), and rendered GeoTiffs in ArcGIS 10.3.1 (ESRI 2015).

253

254 **RESULTS**

255 All traits varied with temperature (Fig. 2), with thermal optima ranging from 23.4ºC for
256 adult lifespan (*lf*) to 33.0ºC for parasite development rate (*PDR*). Unimodal thermal responses
257 were supported for most traits, though declines at high temperatures were not directly observed
258 for biting rate (*a*) and parasite development rate (*PDR*). Instead, data from other mosquito
259 species and ectotherm physiology theory imply that these traits must decline at very high
260 temperatures (~40ºC).

261 The optimal temperature for transmission (relative R_0) peaked near 26.4ºC regardless of
262 whether mosquito density depended on temperature, because optimal transmission aligned with
263 optimal mosquito density (Fig. 3; temperature-dependent *M* model: 26.4ºC, constant *M* model:
264 26.6ºC, mosquito density [*M*]: 26.2ºC). By contrast, the range of temperatures that were suitable

265 for transmission is much narrower when mosquito density depends on temperature because
266 temperature-dependent mosquito density constrains transmission at the thermal limits (Fig. 3;
267 temperature-dependent *M* model: 17.0 – 31.5ºC, constant *M* model: 12.9 – 33.7ºC). Fecundity
268 (*EFD*) and adult lifespan (*lf*) constrain R_0 at the upper thermal limit, while fecundity (*EFD*),
269 larval survival (*pLA*), egg survival (raft viability [*pRH*] and survival within rafts [*nLR*]), and
270 adult lifespan (*lf*) constrain R_0 at the lower thermal limit (Fig. S7). All of these traits (except
271 adult lifespan) only occur in, and adult lifespan is quantitatively more important in, the
272 temperature-dependent *M* model. Correspondingly, uncertainty in these traits generated the most
273 uncertainty in R_0 at the respective thermal limits (Fig. S7C). The intermediate optimal
274 temperature for R_0 was most sensitive to adult mosquito lifespan (Fig. S7). Near the optimum,
275 most uncertainty in R_0 was due to uncertainty in adult lifespan, egg raft viability, and fecundity.
276 Substituting larval traits from alternative vectors or pathogen infection traits for Murray Valley
277 Encephalitis virus did not substantially alter the R_0 thermal response, since *Cx. annulirostris* life
278 history traits strongly constrained transmission (Fig. S5).

279 Temperature suitability for transmission varies seasonally across Australia. In subtropical
280 and temperate locations (Brisbane and further south), low temperatures force R_0 to zero for part
281 of the year (Figs. 4A, 5). Monthly mean temperatures in these areas fall along the increasing
282 portion of the R_0 curve for the entire year, so thermal suitability for RRV transmission increases
283 with temperature in these areas. By contrast, in tropical, northern Australia (Darwin and Cairns),
284 the temperature remains suitable throughout the year (Figs. 4, 5). Darwin is the only major city
285 where mean temperatures are high enough to depress transmission. Most Australians live in
286 southern, temperate areas of the country, making country-scale transmission seasonal; as
287 hypothesized, human cases peak two months after population-weighted $R_0(T)$ (Fig. 6).

288

289 **DISCUSSION**

290 In a warming world, it is critical to understand effects of temperature on transmission of
291 mosquito-borne disease. Characterizing nonlinear thermal responses by identifying transmission
292 optima and limits is useful for predicting geographic, seasonal, and interannual variation in
293 disease. Thermal responses can vary substantially among diseases and vector species (Mordecai
294 *et al.* 2013, 2017), yet we lack mechanistic models based on empirical, unimodal thermal
295 responses for many diseases and vectors. Here, we parameterized a temperature-dependent
296 model for transmission of Ross River virus (Fig. 2) with data from two important vector species
297 (*Cx. annulirostris* and *Ae. vigilax*; Fig. 1). The optimal temperature for disease transmission is
298 moderate (26-27ºC; Fig. 3), and largely determined by the thermal response of adult mosquito
299 lifespan (Fig. S7). Both low and high temperatures limit transmission due to low mosquito
300 fecundity and survival at all life stages (Fig. S7). Temperature explains the geography of year-
301 round endemic versus seasonally epidemic disease (Figs. 4, 5) and accurately predicts the
302 seasonality of human cases at the national scale (Fig. 6). Thus, the empirically-parameterized
303 model for RRV transmission provides a mechanistic link between geographic and seasonal
304 changes in temperature and broad-scale patterns of disease.

305 While the thermal response of RRV transmission generally matched those of other
306 mosquito-borne pathogens, there were some key differences. The moderate optimal temperature
307 for RRV (26-27ºC) fit within the range of thermal optima for other diseases: malaria
308 transmission by *Anopheles* spp. at 25ºC, and dengue and other viruses by *Ae. aegypti* and *Ae.*
309 *albopictus* at 29ºC and 26ºC, respectively (Fig. S6; Mordecai *et al.* 2013, 2017; Johnson *et al.*
310 2015). For all of these diseases, the specific optimal temperature for transmission was largely

311 determined by the thermal response of adult lifespan (Mordecai *et al.* 2013, 2017; Johnson *et al.*
312 2015). However, the traits that limited RRV transmission at high and low temperatures differed
313 from other systems. The lower thermal limit for RRV was most constrained by fecundity and
314 survival at all stages while the upper thermal limit was most constrained by fecundity and adult
315 lifespan. By contrast, the thermal limits for malaria transmission were determined by parasite
316 development rate at cool temperatures and egg-to-adult survival at high temperatures (Mordecai
317 *et al.* 2013). As with previous models, the upper and lower thermal limits of RRV transmission
318 are much more uncertain than the optimum (Fig. 3; Johnson *et al.* 2015; Mordecai *et al.* 2017),
319 because trait responses are inherently harder to measure near their thermal limits where survival
320 is low and development is slow or incomplete. Our results support a general pattern of
321 intermediate thermal optima for transmission where the well-resolved optimal temperature is
322 driven by adult mosquito lifespan, but upper and lower thermal limits are more uncertain and
323 may be determined by unique traits for different vectors and pathogens.

324 We were able to fit thermal responses for all of the traits needed to calculate R_0, but the
325 data were limited in two keys ways. First, two of the traits (fecundity and adult lifespan) had data
326 from only three temperatures. We used priors derived from data from other mosquito species to
327 minimize over-fitting and better represent the true fit and uncertainty in these trait responses
328 (Fig. 2, versus uniform priors in Fig. S1). However, data from more temperatures would increase
329 our confidence in the fitted thermal responses. Second, no RRV vector species had data for all
330 traits (Fig. 1), so we combined mosquito traits from *Cx. annulirostris* and pathogen infection
331 traits in *Ae. vigilax*—two broadly-distributed vector species (Fig. 1)—to build composite R_0
332 models. Geographic and seasonal variation in vector populations suggests that *Ae.*
333 *camptorhynchus* and *Ae. vigilax* have different thermal niches (cooler and warmer, respectively)

334 and *Cx. annulirostris* has a broader thermal niche (Fig. 1; Russell 1998). Temperature-dependent
335 trait data for more species are needed to test the hypothesis that these niches are reflected in the
336 species' thermal responses. If true, predictions based on the model here may not be accurate for
337 transmission by *Ae. camptorhynchus* and *Ae. vigilax*, since the model results are largely
338 determined by *Cx. annulirostris* trait responses. That hypothesis could also explain why RRV
339 persists over a wide climatic and latitudinal gradient. Thermal response experiments with other
340 important RRV vectors are a critical area for future research.

341 The temperature-dependent R_0 model provides a mechanistic explanation for
342 independently-observed patterns of RRV transmission across Australia. As predicted (Figs. 4, 5),
343 RRV is endemic in tropical Australia and epidemic in subtropical and temperate Australia
344 (Weinstein 1997). The model also accurately predicts the seasonality of cases at the national
345 scale (Fig. 6), reproducing the *a priori* predicted lag of 8-10 weeks for temperature to affect
346 reported human cases (Hu *et al.* 2006; Jacups *et al.* 2008b; Stewart Ibarra *et al.* 2013; Mordecai
347 *et al.* 2017). Further, as temperatures increase from spring into summer, RRV transmission by
348 *Cx. annulirostris* in inland areas often moves south along the latitudinal gradient (Russell 1998),
349 matching the model prediction (Fig. 5). Although temperature is often invoked as a potential
350 driver for such patterns, it is difficult to establish causality from statistical inference alone,
351 particularly if temperature and disease both exhibit strong seasonality and therefore could both
352 be responding to another latent driver (Sugihara *et al.* 2012). Thus, the mechanistic model is a
353 critical piece of evidence linking temperature to patterns of disease.

354 In addition to explaining broad-scale patterns of RRV disease, the unimodal thermal
355 model explains previously contradictory local-scale results. Specifically, statistical evidence for
356 temperature impacts on local time series of RRV cases is mixed. RRV incidence is often—but

357 not always—positively associated with warmer temperatures (Tong & Hu 2001; Tong *et al.*
358 2002, 2004, Hu *et al.* 2004, 2010; Jacups *et al.* 2008b; Williams *et al.* 2009; Werner *et al.* 2012;
359 Koolhof *et al.* 2017). However, variation in temperature impacts across local time series is
360 expected from the intermediate thermal optimum for transmission, since the optimum is near
361 observed mean temperatures in tropical and sub-tropical climates. The strongest statistical signal
362 of temperature on disease is expected to occur in temperate regions where mean temperature
363 varies along the rapidly rising portion of the R_0 curve (~20-26°C). If mean temperatures vary
364 both above and below the optimum (as in Darwin), important effects of temperature may be
365 masked in time series models that fit linear responses. Additionally, if temperatures are always
366 relatively suitable (as in tropical climates) or unsuitable (as in very cool temperate climates),
367 variation in disease may be due primarily to other factors. A nonlinear mechanistic model is
368 critical for estimating impacts of temperature on transmission because the effect of increasing
369 temperature by a few degrees can have a positive, negligible, or negative impact on R_0 along
370 different parts of the thermal response curve. Although field-based evidence for unimodal
371 thermal responses in vector-borne disease is rare (but see Mordecai *et al.* 2013; Peña-García *et*
372 *al.* 2017), there is some evidence for high temperatures constraining RRV transmission and
373 vector populations: outbreaks were less likely with more days above 35ºC in one area in
374 Queensland (Gatton *et al.* 2005) and populations of *Cx. annulirostris* peaked at 25ºC and
375 declined above 32ºC in Victoria (Dhileepan 1996). Future statistical analyses of RRV cases may
376 benefit from using a nonlinear estimate of temperature-dependent R_0 as a predictor instead of raw
377 temperature (Fig. 5B versus 5A).
378 Aquatic breeding habitat availability is also an important driver of mosquito abundance
379 and mosquito-borne disease. Local rainfall and river flow have been linked to the abundance of

380 RRV vector species (Tall *et al.* 2014) and RRV disease cases (Tong & Hu 2001, 2002b; Hu *et al.*
381 2004; Kelly-Hope *et al.* 2004a; Tong *et al.* 2004; Gatton *et al.* 2005; Jacups *et al.* 2008b; Bi *et al.*
382 2009; Williams *et al.* 2009; Werner *et al.* 2012), as have unusually high tides in coastal areas
383 with saltmarsh mosquitoes (Tong & Hu 2002a; Tong *et al.* 2004; Jacups *et al.* 2008b).
384 Overlaying models of species-specific breeding habitat with temperature-dependent models
385 would better resolve the geographic and seasonal distribution of RRV transmission. R_0 peaked at
386 similar temperatures whether or not we assumed that mosquito abundance was temperature-
387 dependent (eq. 1 versus eq. 2); however, the range of suitable temperatures was much wider for
388 the model that assumed a temperature-independent mosquito population (Fig. 3). Since breeding
389 habitat availability can only impact vector populations when temperatures do not exclude them,
390 it is critical to consider thermal constraints on mosquito abundance even when breeding habitat is
391 considered a stronger driver. Nonetheless, many mechanistic models of temperature-dependent
392 transmission of vector-borne disease do not include thermal effects on vector density (e.g., Paull
393 *et al.* 2017). Our results demonstrate that the decision to include—or exclude—these
394 relationships can have a critical impact on the model results, especially near thermal limits.
395 Several important gaps remain in our understanding of RRV thermal ecology. First, we
396 need better trait thermal response data, for more vector species. Second, the R_0 model needs to be
397 more rigorously validated using time series of human cases to determine the importance of
398 temperature at finer spatiotemporal scales. These analyses should incorporate daily and seasonal
399 temperature variation (Paaijmans *et al.* 2010) and integrate species-specific drivers of breeding
400 habitat availability, like seasonal rainfall and tidal patterns. Finally, translating environmental
401 suitability for mosquito transmission into human cases also depends on past and current disease
402 dynamics in reservoir host and human populations, and their impacts on population immunity.

403 For instance, in Western Australia when recruitment of susceptible juvenile kangaroos is low due
404 to low rainfall in the preceding winter, heavy summer rains may fail to initiate RRV epidemics
405 (Mackenzie *et al.* 2000). By contrast, large outbreaks occur in southeastern Australia when high
406 rainfall follows a dry year, presumably from increased transmission within previously unexposed
407 reservoir populations (Woodruff *et al.* 2002). Building vector species-specific R_0 models and
408 integrating thermal ecology with other drivers are important next steps for accurately forecasting
409 variation in RRV transmission.

410 Extending the results of the temperature-dependent model for RRV transmission to future
411 climate regimes highlights the importance of characterizing nonlinear thermal responses. Climate
412 warming is likely to increase the geographic and seasonal range of transmission potential in
413 temperate, southern Australia where the majority of Australians live. However, climate change is
414 likely to decrease transmission potential in tropical cities like Darwin, where moderate warming
415 (~3ºC) would push temperatures above the upper thermal limit for transmission for most of the
416 year (Fig. 5). However, the extent of climate-driven declines in transmission will depend on how
417 much *Cx. annulirostris* and *Ae. vigilax* can adapt to extend their upper thermal limits and
418 whether warmer-adapted mosquito species (e.g., *Ae. aegypti* and potentially *Ae. polynesiensis*)
419 can invade and sustain RRV transmission cycles. Thus, while the response of RRV transmission
420 by current vector species to climate change is predictable based on vector and parasite trait
421 thermal responses, future RRV disease dynamics will also depend on vector adaptation, potential
422 vector species invasions, and climate change impacts on sea level and precipitation that drive
423 vector habitat availability.

424

425 **ACKNOWLEDGEMENTS**

We thank Leah Johnson and Matt Thomas for helpful comments and Cameron Webb for originally posting the RRV case data (https://cameronwebb.wordpress.com/2014/04/09/why-is-mosquito-borne-disease-risk-greater-in-autumn/). All authors were supported by the National Science Foundation (DEB-1518681; https://nsf.gov/). EAM was supported by the NSF (DEB-1640780; https://nsf.gov/), the Stanford Woods Institute for the Environment (https://woods.stanford.edu/research/environmental-venture-projects), and the Stanford Center for Innovation in Global Health (http://globalhealth.stanford.edu/research/seed-grants.html).

REFERENCES

Angilletta, M.J. (2009). *Thermal Adaptation: A Theoretical and Empirical Synthesis*. Oxford University Press.

Aubry, M., Finke, J., Teissier, A., Roche, C., Broult, J., Paulous, S., *et al.* (2015). Silent circulation of ross river virus in French Polynesia. *Int. J. Infect. Dis.*, 37, e19–e24.

Australian Bureau of Statistics. (2017). *3218.0 - Regional Population Growth, Australia, 2016*. Canberra.

Barton, P.S., Aberton, J.G. & Kay, B.H. (2004). Spatial and temporal definition of *Ochlerotatus camptorhynchus* (Thomson) (Diptera: Culicidae) in the Gippsland Lakes system of eastern Victoria. *Aust. J. Entomol.*, 43, 16–22.

Bi, P., Hiller, J.E., Cameron, a S., Zhang, Y. & Givney, R. (2009). Climate variability and Ross River virus infections in Riverland, South Australia, 1992-2004. *Epidemiol. Infect.*, 137, 1486–93.

Biggs, A.J.W. & Mottram, P. (2008). Links between dryland salinity, mosquito vectors, and Ross River Virus disease in southern inland Queensland—an example and potential implications. *Soil Res.*, 46, 62–66.

Bivand, R., Keitt, T. & Rowlingson, B. (2017). rgdal: Bindings for the "Geospatial" Data Abstraction Library.

Bivand, R. & Lewin-Koh, N. (2017). maptools: Tools for Reading and Handling Spatial Objeccts.

Brière, J.-F., Pracros, P., Le Roux, A.-Y. & Pierre, J.-S. (1999). A Novel Rate Model of Temperature-Dependent Development for Arthropods. *Environ. Entomol.*, 28, 22–29.

Brokenshire, T., Symonds, D., Reynolds, R., Doggett, S., Geary, M. & Russell, R. (2000). A cluster of locally-acquired Ross River virus infection in outer western Sydney. *NSW Public Heal. Bull*, 11, 132–134.

Campbell, J., Aldred, J. & Davis, G. (1989). Some aspects of the natural history of Ross River virus in south east Gippsland, Victoria. *Arbovirus Res. Aust.*, 5, 24–28.

Carver, S., Spafford, H., Storey, A. & Weinstein, P. (2009). Dryland Salinity and the Ecology of Ross River Virus: The Ecological Underpinnings of the Potential for Transmission. *Vector-Borne Zoonotic Dis.*, 9, 611–622.

Claflin, S.B. & Webb, C.E. (2015). Ross River Virus: Many Vectors and Unusual Hosts Make for an Unpredictable Pathogen. *PLoS Pathog.*, 11, 1–6.

Clements, A.N. & Paterson, G.D. (1981). The Analysis of Mortality and Survival Rates in Wild Populations of Mosquitoes. *J. Appl. Ecol.*, 18, 373–399.

Dell, A.I., Pawar, S. & Savage, V.M. (2011). Systematic variation in the temperature dependence of physiological and ecological traits. *Proc. Natl. Acad. Sci.*, 108, 10591–10596.

Dhileepan, K. (1996). Mosquito seasonality and arboviral disease incidence in Murray valley, southeast Australia. *Med. Vet. Entomol.*, 10, 375–384.

Dietz, K. (1993). The estimation of the basic reproduction number for infectious diseases. *Stat. Methods Med. Res.*, 2, 23–41.

ESRI. (2015). ArcGIS Desktop.

Faull, K.J. & Williams, C.R. (2016). Differentiation of *Aedes aegypti* and *Aedes notoscriptus* (Diptera: Culicidae) eggs using scanning electron microscopy. *Arthropod Struct. Dev.*, 45, 273–280.

Flies, E.J., Lau, C.L., Carver, S. & Weinstein, P. (2018). Another Emerging Mosquito-Borne Disease? Endemic Ross River Virus Transmission in the Absence of Marsupial Reservoirs. *Bioscience*.

Frances, S.P., Cooper, R.D., Rowcliffe, K.L., Chen, N. & Cheng, Q. (2004). Occurrence of Ross River virus and Barmah Forest virus in mosquitoes at Shoalwater Bay military training area, Queensland, Australia. *J. Med. Entomol.*, 41, 115–20.

GADM. (2012). GADM database of Global Administrative Boundaries, version 2.0.

485 Gatton, M.L., Kay, B.H. & Ryan, P.A. (2005). Environmental predictors of Ross River virus
486 disease outbreaks in Queensland, Australia. *Am J Trop Med Hyg*, 72, 792–799.
487 Harley, D., Ritchie, S., Phillips, D. & van den Hurk, A. (2000). Mosquito isolates of Ross River
488 virus from Cairns, Queensland, Australia. *Am. J. Trop. Med. Hyg.*, 62, 561–5.
489 Harley, D., Sleigh, A. & Ritchie, S. (2001). Ross River Virus Transmission, Infection, and
490 Disease: a Cross-Disciplinary Review. *Clin. Microbiol. Rev.*, 14, 909–932.
491 Hijmans, R.J. (2016). raster: Geographic Data Analysis and Modeling.
492 Hu, W., Clements, A., Williams, G., Tong, S. & Mengersen, K. (2010). Bayesian spatiotemporal
493 analysis of socio-ecologic drivers of Ross River virus transmission in Queensland,
494 Australia. *Am. J. Trop. Med. Hyg.*, 83, 722–728.
495 Hu, W., Nicholls, N., Lindsay, M., Dale, P., McMichael, A.J., Mackenzie, J.S., *et al.* (2004).
496 Development of a predictive model for ross river virus disease in Brisbane, Australia. *Am J*
497 *Trop Med Hyg*, 71, 129–137.
498 Hu, W., Tong, S., Mengersen, K., Oldenburg, B. & Dale, P. (2006). Mosquito species (Diptera:
499 Culicidae) and the transmission of Ross River virus in Brisbane, Australia. *J. Med.*
500 *Entomol.*, 43, 375–381.
501 Jacups, S.P., Carter, J., Kurucz, N., McDonnell, J. & Whelan, P.I. (2015). Determining
502 meteorological drivers of salt marsh mosquito peaks in tropical northern Australia. *J. Vector*
503 *Ecol.*, 40, 277–281.
504 Jacups, S.P., Whelan, P.I. & Currie, B.J. (2008a). Ross River virus and Barmah Forest virus
505 infections: a review of history, ecology, and predictive models, with implications for
506 tropical northern Australia. *Vector-borne Zoonotic Dis.*, 8, 283–297.
507 Jacups, S.P., Whelan, P.I., Markey, P.G., Cleland, S.J., Williamson, G.J. & Currie, B.J. (2008b).
508 Predictive indicators for Ross River virus infection in the Darwin area of tropical northern
509 Australia, using long-term mosquito trapping data. *Trop. Med. Int. Heal.*, 13, 943–952.
510 Johnson, L.R., Ben-Horin, T., Lafferty, K.D., McNally, A., Mordecai, E., Paaijmans, K.P., *et al.*
511 (2015). Understanding uncertainty in temperature effects on vector-borne disease: A
512 Bayesian approach. *Ecology*, 96, 203–213.
513 Kay, B.H. & Jennings, C.D. (2002). Enhancement or Modulation of the Vector Competence of
514 *Ochlerotatus vigilax* (Diptera: Culicidae) for Ross River Virus by Temperature. *J. Med.*
515 *Entomol.*, 39, 99–105.

516 Kelly-Hope, L.A., Purdie, D.M. & Kay, B.H. (2004a). Differences in Climatic Factors Between
517 Ross River Virus Disease Outbreak and Nonoutbreak Years. *J. Med. Entomol*, 41, 1116–
518 1122.
519 Kelly-Hope, L.A., Purdie, D.M. & Kay, B.H. (2004b). Ross river virus disease in Australia,
520 1886-1998, with analysis of risk factors associated with outbreaks. *J. Med. Entomol.*, 41,
521 133–150.
522 Klapsing, P., MacLean, J.D., Glaze, S., McClean, K.L., Drebot, M.A., Lanciotti, R.S., *et al.*
523 (2005). Ross river virus disease reemergence, Fiji, 2003-2004. *Emerg. Infect. Dis.*, 11, 613–
524 615.
525 Kokkinn, M.J., Duval, D.J. & Williams, C.R. (2009). Modelling the ecology of the coastal
526 mosquitoes *Aedes vigilax* and *Aedes camptorhynchus* at Port Pirie, South Australia. *Med.*
527 *Vet. Entomol.*, 23, 85–91.
528 Koolhof, I.S., Bettiol, S. & Carver, S. (2017). Fine-temporal forecasting of outbreak probability
529 and severity: Ross River virus in Western Australia. *Epidemiol. Infect.*, 145, 2949–2960.
530 Koolhof, I.S. & Carver, S. (2017). Epidemic host community contribution to mosquito-borne
531 disease transmission: Ross River virus. *Epidemiol. Infect.*, 145, 656–666.
532 Lau, C., Aubry, M., Musso, D., Teissier, A., Paulous, S., Desprès, P., *et al.* (2017). New
533 evidence for endemic circulation of Ross River virus in the Pacific Islands and the potential
534 for emergence. *Int. J. Infect. Dis.*, 57, 73–76.
535 Lindsay, M., Condon, R., Mackenzie, J., Johansen, C., D'Ercole, M. & Smith, D. (1992). A
536 major ourbreak of Ross river virus infection in the south-west of Western Australia and the
537 Perth metropolitan area. *Comm. Dis. Int.*, 16, 290–294.
538 Lindsay, M., Oliveira, N., Jasinska, E., Johansen, C., Harrington, S., Wright, A.E., *et al.* (1996).
539 An outbreak of Ross River virus disease in Southwestern Australia. *Emerg. Infect. Dis.*, 2,
540 117–120.
541 Lindsay, M.D.A., Broom, A.K., Wright, A.E. (Tony), Johansen, C.A. & Mackenzie, J.S. (1993a).
542 Ross River Virus Isolations from Mosquitoes in Arid Regions of Western Australia:
543 Implication of Vertical Transmission as a Means of Persistence of the Virus. *Am. J. Trop.*
544 *Med. Hyg.*, 49, 686–696.
545 Lindsay, M.D.A., Jardine, A., Johansen, C.A., Wright, A.E., Harrington, S.A. & Weinstein, P.
546 (2007). Mosquito (Diptera: Culicidae) fauna in inland areas of south-west Western

Australia. *Aust. J. Entomol.*, 46, 60–64.

Lindsay, M.D., Johansen, C., Broom, A.K., D'Ercole, M., Wright, A.E., Condon, R., *et al.* (1993b). The epidemiology of outbreaks of Ross River virus infection in Western Australia in 1991–1992. *Arbovirus Res. Aust.*, 6, 72–76.

Liu-Helmersson, J., Stenlund, H., Wilder-Smith, A. & Rocklöv, J. (2014). Vectorial capacity of *Aedes aegypti*: Effects of temperature and implications for global dengue epidemic potential. *PLoS One*, 9.

MacDonald, G. (1952). The Analysis of Sporozoite Rate. *Trop. Dis. Bull.*, 49, 569–586.

Mackenzie, J.S., Lindsay, M.D. & Broom, A.K. (2000). The effect of climate and weather on the transmission of Ross River and Murray Valley encephalitis viruses. *Microbiol. Aust.*, 21, 20–25.

McDonald, G., McLaren, I.W., Shelden, G.P. & Smith, I.R. (1980). The effect of temperature on the population growth potential of *Culex annulirostris* Skuse (Diptera: Culicidae). *Aust. J. Ecol.*, 5, 379–384.

McDonnell, L., Kolbe, T., Carvan, T. & Gilchrist, K. (1994). Outbreak of Ross River virus disease in the south west districts of NSW, summer 1993. *New South Wales Public Heal. Bull.*, 5, 98–9.

McManus, T.J., Russell, R.C., Wells, P.J., Clanc, J.G., Fennell, M. & Cloonan, M.J. (1992). Further studies on the epidemiology and effects of Ross River virus in Tasmania. *Arbovirus Res. Aust.*, 6, 68–72.

Merianos, A., Farland, A.M., Patel, M., Currie, B., Whelan, P., Dentith, H., *et al.* (1992). A concurrent outbreak of Barmah Forest and Ross River virus disease in Nhulunbuy, Northern Territory. *Commun. Dis. Intell.*, 16, 110–111.

Mordecai, E.A., Cohen, J.M., Evans, M. V., Gudapati, P., Johnson, L.R., Lippi, C.A., *et al.* (2017). Detecting the impact of temperature on transmission of Zika, dengue, and chikungunya using mechanistic models. *PLoS Negl. Trop. Dis.*, 11, e0005568.

Mordecai, E.A., Paaijmans, K.P., Johnson, L.R., Balzer, C., Ben-Horin, T., de Moor, E., *et al.* (2013). Optimal temperature for malaria transmission is dramatically lower than previously predicted. *Ecol. Lett.*, 16, 22–30.

Mottram, P., Kay, B.H. & Kettle, D.S. (1986). The effect of temperature on eggs and immature Stages of *Culex annulirostris* Skuse (Diptera: Culicidae). *Aust. J. Entomol.*, 25, 131–136.

578 Paaijmans, K.P., Blanford, S., Bell, A.S., Blanford, J.I., Read, A.F. & Thomas, M.B. (2010).
579 Influence of climate on malaria transmission depends on daily temperature variation. *Proc.*
580 *Natl. Acad. Sci. U. S. A.*, 107, 15135–9.
581 Parham, P.E. & Michael, E. (2010). Modeling the effects of weather and climate change on
582 malaria transmission. *Environ. Health Perspect.*, 118, 620–626.
583 Paull, S.H., Horton, D.E., Ashfaq, M., Rastogi, D., Kramer, L.D., Diffenbaugh, N.S., *et al.*
584 (2017). Drought and immunity determine the intensity of West Nile virus epidemics and
585 climate change impacts. *Proc. R. Soc. B Biol. Sci.*, 284, 20162078.
586 Peña-García, V.H., Triana-Chávez, O. & Arboleda-Sánchez, S. (2017). Estimating Effects of
587 Temperature on Dengue Transmission in Colombian Cities. *Ann. Glob. Heal.*, 83, 509–518.
588 Plummer, M. (2003). JAGS: A program for analysis of Bayesian graphical models using Gibbs
589 sampling. *Proc. 3rd Int. Work. Distrib. Stat. Comput.*, 1–10.
590 R Core Team. (2017). *R: A language and for statistical computing*. R Foundation for Statistical
591 Computing, Vienna, Austria.
592 Rae, D.J. (1990). Survival and development of the immature stages of *Culex annulirostris*
593 (Diptera: Culicidae) at the Ross River Dam in tropical eastern Australia. *J Med Entomol*,
594 27, 756–762.
595 Ritchie, S.A., Fanning, I.D., Phillips, D.A., Standfast, H.A., Mcginn, D. & Kay, B.H. (1997).
596 Ross River Virus in Mosquitoes (Diptera: Culicidae) During the 1994 Epidemic Around
597 Brisbane, Australia. *J. Med. Entomol.*, 34, 156–159.
598 Rogers, D.J. & Randolph, S.E. (2006). Climate Change and Vector-Borne Diseases. *Adv.*
599 *Parasitol.*, 62, 345–381.
600 Rosen, L., Gubler, D.J. & Bennett, P.H. (1981). Epidemic Polyarthritis (Ross River) Virus
601 Infection in the Cook Islands. *Am. J. Trop. Med. Hyg.*, 30, 1294–1302.
602 Russell, R.C. (1986). *Culex Annulirostris* Skuse (Diptera: Culicidae) at Appin, N.S.W.—
603 bionomics and behavior. *Aust. J. Entomol.*, 25, 103–109.
604 Russell, R.C. (1994). Ross River virus: disease trends and vector ecology in Australia. *Bull. Soc.*
605 *Vector Ecol.*, 19, 73–81.
606 Russell, R.C. (1998). Mosquito-borne arboviruses in Australia: the current scene and
607 implications of climate change for human health. *Int. J. Parasitol.*, 28, 955–969.
608 Russell, R.C. (2002). Ross River Virus: Ecology and Distribution. *Ann. Rev. Entomol.*, 47, 1–31.

Russell, R.C., Cloonan, M.J., Wells, P.J. & Vale, T.G. (1991). Mosquito (Diptera: Culicidae) and Arbo virus Activity on the South Coast of New South Wales, Australia, in 1985–1988. *J. Med. Entomol.*, 28, 796–804.

Ryan, P.A., Do, K.-A. & Kay, B.H. (2000). Definition of Ross River Virus Vectors at Maroochy Shire, Australia. *J. Med. Entomol.*, 37, 146–152.

Schmaedick, M.A., Ball, T.S., Burkot, T.R. & Gurr, N.E. (2008). Evaluation of Three Traps for Sampling *Aedes polynesiensis* and Other Mosquito Species in American Samoa 1. *J. Am. Mosq. Control Assoc.*, 24, 319–322.

Shocket, M.S., Anderson, C.B., Caldwell, J.M., Childs, M.L., Han, S., Harris, M.J., *et al.* (n.d.). Environmental Drivers of Vector-borne Diseases. In: *Ecology of Vector-borne Diseases* (ed. Drake, J.M.).

Siraj, A.S., Bouma, M.J., Santos-Vega, M., Yeshiwondim, A.K., Rothman, D.S., Yadeta, D., *et al.* (2015). Temperature and population density determine reservoir regions of seasonal persistence in highland malaria. *Proc. R. Soc. B Biol. Sci.*, 282, 20151383.

Stephenson, E.B., Peel, A.J., Reid, S.A., Jansen, C.C. & McCallum, H. (2018). The non-human reservoirs of Ross River virus: a systematic review of the evidence. *Parasit. Vectors*, 11, 188.

Stewart Ibarra, A.M. & Lowe, R. (2013). Climate and non-climate drivers of dengue epidemics in southern coastal Ecuador. *Am. J. Trop. Med. Hyg.*, 88, 971–981.

Stewart Ibarra, A.M., Ryan, S.J., Beltrán, E., Mejía, R.L., Silva, M., Muñoz, Á., *et al.* (2013). Dengue Vector Dynamics (*Aedes aegypti*) Influenced by Climate and Social Factors in Ecuador: Implications for Targeted Control. *PLoS One*, 8, e78263.

Su, Y.-S. & Yajima, M. (2009). R2jags: A Package for Running jags from R.

Sugihara, G., May, R., Ye, H., Hsieh, C. -h., Deyle, E., Fogarty, M., *et al.* (2012). Detecting Causality in Complex Ecosystems. *Science (80-.).*, 338, 496–500.

Tall, J.A., Gatton, M.L. & Tong, S. (2014). Ross River Virus Disease Activity Associated With Naturally Occurring Nontidal Flood Events in Australia: A Systematic Review. *J. Med. Entomol.*, 51, 1097–1108.

Tong, S., Bi, P., Donald, K. & McMichael, A.J. (2002). Climate variability and Ross River virus transmission. *J. Epidemiol. Community Heal.*, 56, 617–621.

Tong, S. & Hu, W. (2001). Climate variation and incidence of Ross River virus in Cairns,

640 Australia: a time-series analysis. *Environ. Health Perspect.*, 109, 1271–1273.
641 Tong, S. & Hu, W. (2002a). Different responses of Ross River virus to climate. *Occup Env. Med*,
642 59, 739–744.
643 Tong, S. & Hu, W. (2002b). Different responses of Ross River virus to climate variability
644 between coastline and inland cities in Queensland, Australia. *Occup Env. Med*, 59, 739–
645 744.
646 Tong, S., Hu, W. & McMichael, A.J. (2004). Climate variability and Ross River virus
647 transmission in Townsville Region, Australia, 1985-1996. *Trop. Med. Int. Heal.*, 9, 298–
648 304.
649 Weinstein, P. (1997). An ecological approach to public health intervention: Ross River virus in
650 Australia. *Env. Heal. Perspect*, 105, 364–366.
651 Werner, a. K., Goater, S., Carver, S., Robertson, G., Allen, G.R. & Weinstein, P. (2012).
652 Environmental drivers of Ross River virus in southeastern Tasmania, Australia: towards
653 strengthening public health interventions. *Epidemiol. Infect.*, 140, 359–371.
654 Wesolowski, A., Qureshi, T., Boni, M.F., Sundsøy, P.R., Johansson, M.A., Rasheed, S.B., *et al.*
655 (2015). Impact of human mobility on the emergence of dengue epidemics in Pakistan. *Proc.*
656 *Natl. Acad. Sci.*, 201504964.
657 Whelan, P.I., Krause, V., Horsburgh, K., Sutherland, G. & Rossiter, J. (1995). Confirmed case of
658 Ross River virus infection acquired in Alice Springs March 1995. *North. Territ. Commun.*
659 *Dis. Bull.*, 2, 9–11.
660 Whelan, P.I., Merianos, A., Hayes, G. & Krause, V. (1997). Ross River Virus Transmission in
661 Darwin, Northern Territory, Australia. *Arbovirus Res. Aust.*, 7, 337–345.
662 Whelan, P.I., Merianos, A., Patel, M.S., Tai, K.S. & Currie, B. (1992). The epidemiology of
663 arbovirus infection in the Northern Territory 1980-92. *Arbovirus Res. Aust.*, 6, 266–70.
664 Williams, C.R., Fricker, S.R. & Kokkinn, M.J. (2009). Environmental and entomological factors
665 determining Ross River virus activity in the River Murray Valley of South Australia. *Aust.*
666 *N. Z. J. Public Health*, 33, 284–288.
667 Woodruff, R.E., Guest, C.S., Garner, M.G., Becker, N., Lindesay, J., Carvan, T., *et al.* (2002).
668 Predicting Ross River virus epidemics from regional weather data. *Epidemiology*, 13, 384–
669 393.
670

SUPPORTING INFORMATION

Additional Supporting Information may be downloaded via the online version of this article at Wiley Online Library (www.ecologyletters.com)

675 **FIGURE 1: Vector species implicated in RRV outbreaks.** Map of Australia and Pacific
676 Islands showing outbreaks of RRV disease in which specific mosquito species were identified as
677 vectors based on the collection of field specimens. Only the six most important species are
678 included. Grid indicates thermal response data availability for each trait in the R_0 model for the
679 five Australian species. Data sources are listed in Table S1.
680
681 **FIGURE 2**: **Thermal responses of *Cx. annulirostris* and Ross River virus (in *Ae. vigilax*)**
682 **traits that drive transmission**. Functions were fit using Bayesian inference with priors fit using
683 data from other mosquito species and viruses. For (E) fecundity and (C) adult lifespan, points
684 show data means and error bars indicate standard error. Black solid lines are posterior
685 distribution means; dashed red lines are 95% credible intervals.
686
687 **FIGURE 3**: **Thermal response of relative R_0**. (A) Posterior means of relative R_0 across
688 temperature. Constant *M* model (eq. 1) assumes mosquito density does not depend on
689 temperature (light blue), while temperature-dependent *M* model (eq. 2) accounts for temperature-
690 dependence of mosquito life history traits (dark blue). Predicted mosquito density (*M*) is also
691 shown for comparison (red). The y-axis illustrates relative R_0 (or *M*) across temperatures rather
692 than absolute values, which would require information about additional drivers and vary across
693 transmission settings. Histograms of (B) the critical thermal minimum, (C) thermal optimum,
694 and (D) critical thermal maximum temperatures for both R_0 models (constant *M*: light blue;
695 temperature-dependent *M*: dark blue).
696

697 **FIGURE 4**: **Transmission potential for Ross River virus based on monthly mean**
698 **temperatures**. Color indicates the number of months of where (A) relative R_0>0 and (B) relative
699 R_0>0.5. Model predictions are based on the median posterior probability for relative R_0. Points
700 indicate selected cities (from Fig. 5), scaled by the percent of the total Australian population
701 residing in each city.
702
703 **FIGURE 5**: **Average seasonality of temperature and predicted temperature-dependent**
704 **relative R_0 in Australian cities.** The selected cities span a latitude and temperature gradient
705 (Darwin = dark red, Cairns = red, Brisbane = dark orange, Perth = light orange, Sydney = aqua,
706 Melbourne = blue, Hobart = dark blue). The sequence of months begins in July and ends in June
707 (both during austral winter). (A) Mean monthly temperatures. Gray shaded areas show
708 temperature at outer 95% CI (light gray), median (medium gray), and inner 95% CI (dark gray)
709 for thresholds where R_0>0. Dashed gray line shows median temperature for R_0 optimum. (B)
710 Relative R_0 as a function of temperature in each city.
711
712 **Figure 6: Seasonality of temperature-dependent relative R_0 (line) and RRV infections**.
713 Human cases (bars) are aggregated nationwide from 1992-2013. Temperature-dependent R_0
714 (line) is weighted by population, calculated from the 15 largest cities in Australia (76.6% of the
715 total population). The sequence of months begins in July and ends in June (during austral
716 winter). Cases peak two months after $R_0(T)$, the *a priori* expected lag between temperature and
717 reported cases.

718 **FIGURE 1**

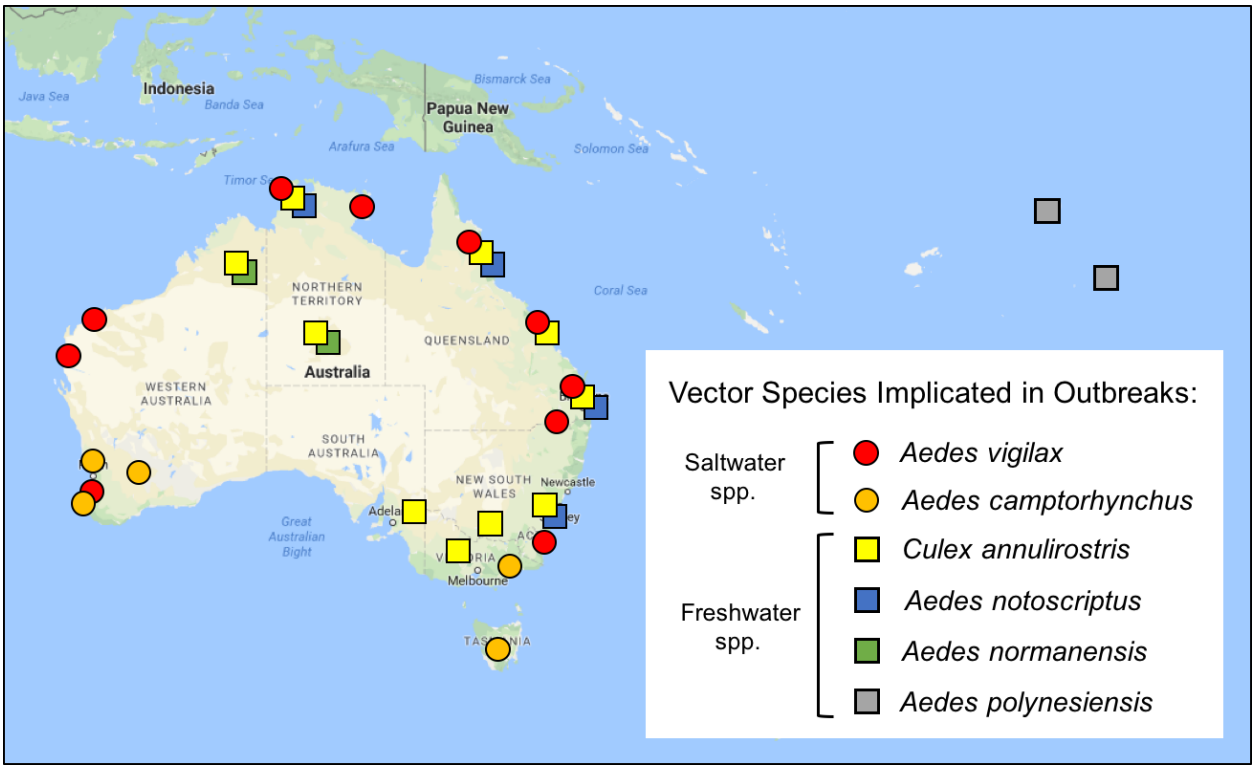

719

Vector / Trait	*a*	*EFD*	*MDR*	p_{EA}	μ	*bc*	*PDR*
Ae. vigilax							
Ae. camptorhynchus							
Cx. annulirostris							
Ae. notoscriptus							
Ae. normanensis							

Data
No Data

720

721

FIGURE 2

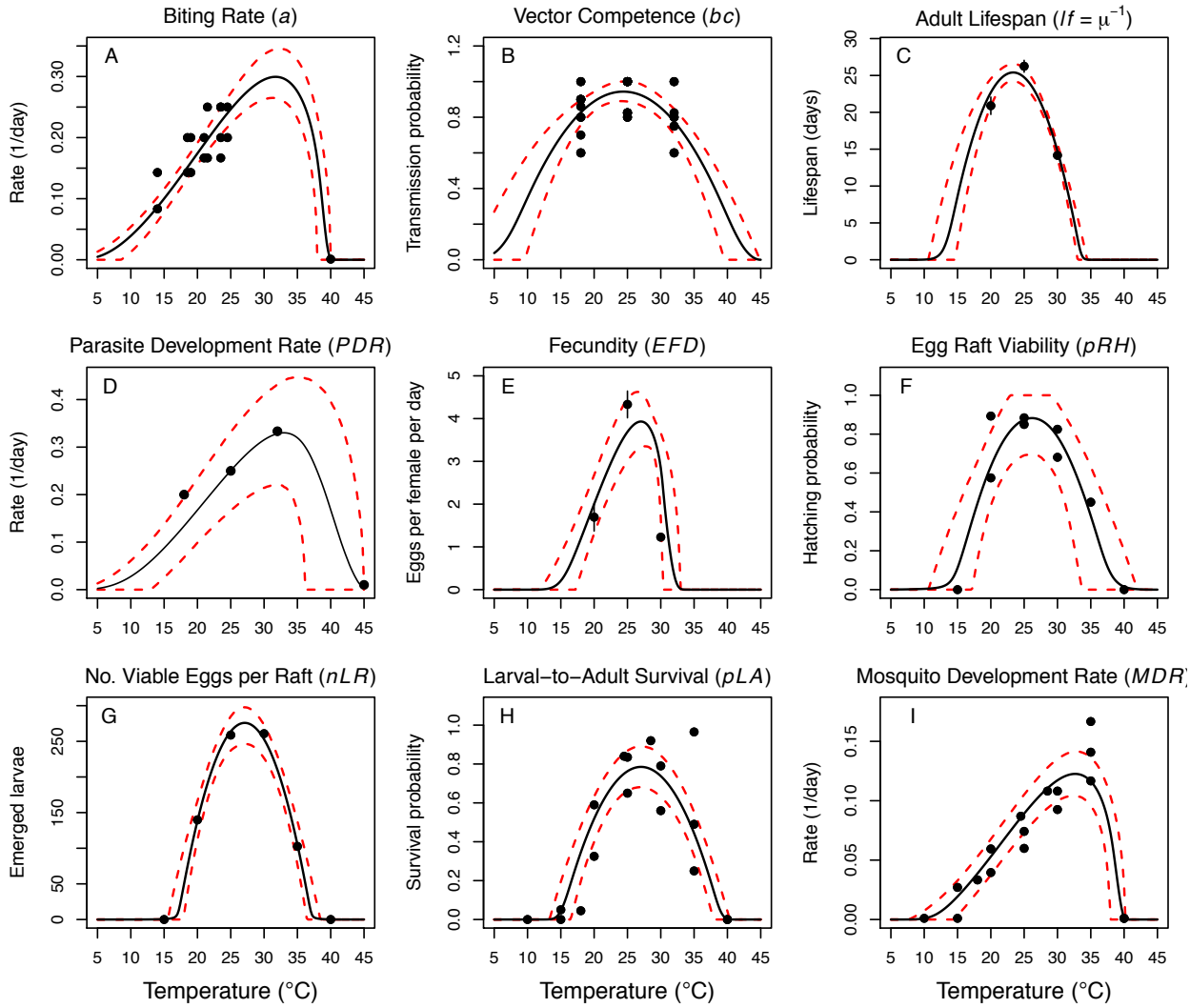
Biting Rate (a)
A
Rate (1/day)
Vector Competence (bc)
B
Transmission probability
Adult Lifespan (lf = μ^-1)
C
Lifespan (days)
Parasite Development Rate (PDR)
D
Rate (1/day)
Fecundity (EFD)
E
Eggs per female per day
Egg Raft Viability (pRH)
F
Hatching probability
No. Viable Eggs per Raft (nLR)
G
Emerged larvae
Larval–to–Adult Survival (pLA)
H
Survival probability
Mosquito Development Rate (MDR)
I
Rate (1/day)
Temperature (°C)
Temperature (°C)
Temperature (°C)

FIGURE 3

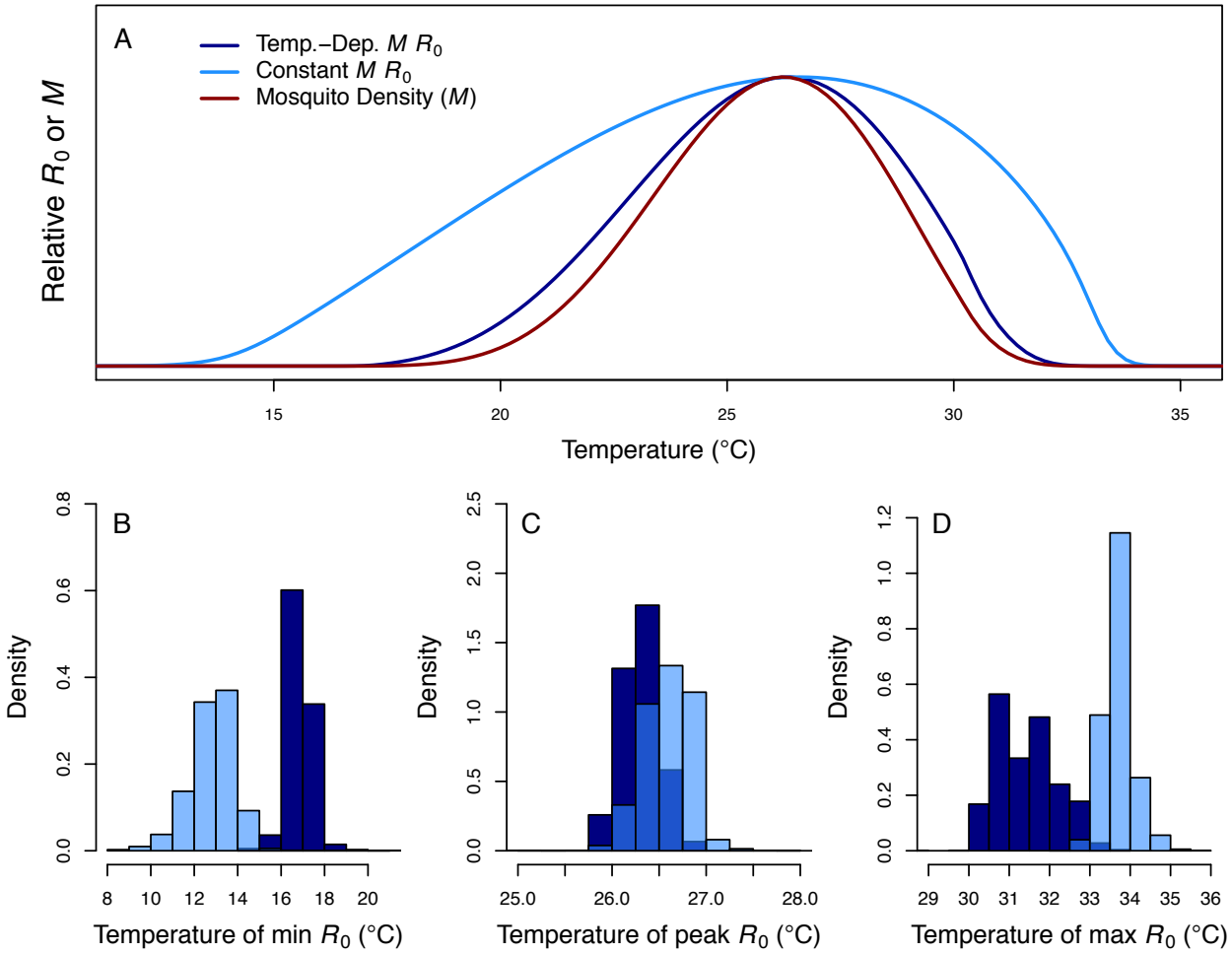
A
Temp.–Dep. M R_0
Constant M R_0
Mosquito Density (M)
Relative R_0 or M
15
20
25
30
35
Temperature (°C)
B
Density
0.0
0.2
0.4
0.6
0.8
8
10
12
14
16
18
20
Temperature of min R_0 (°C)
C
Density
0.0
0.5
1.0
1.5
2.0
2.5
25.0
26.0
27.0
28.0
Temperature of peak R_0 (°C)
D
Density
0.0
0.2
0.4
0.6
0.8
1.0
1.2
29
30
31
32
33
34
35
36
Temperature of max R_0 (°C)

FIGURE 4

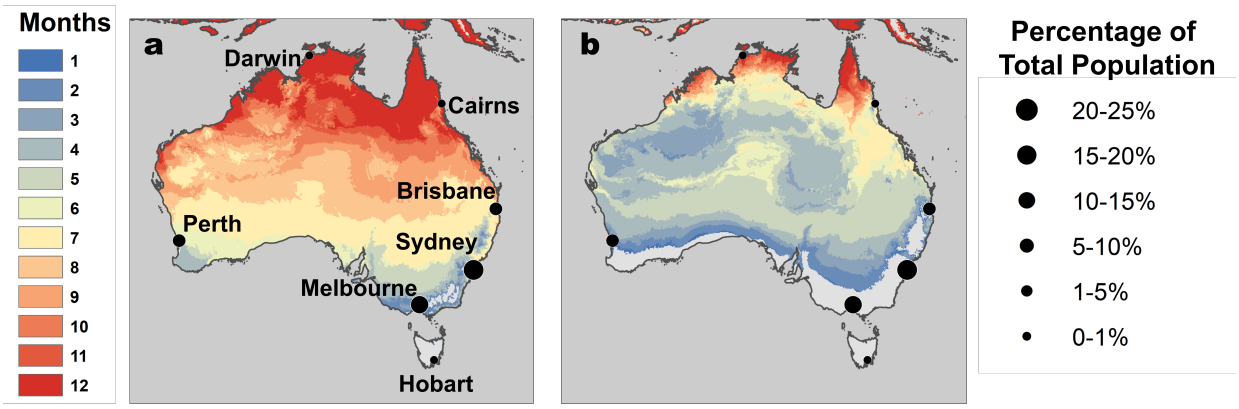
Months
1
2
3
4
5
6
7
8
9
10
11
12
a
Darwin
Cairns
Brisbane
Perth
Sydney
Melbourne
Hobart
b
Percentage of Total Population
20-25%
15-20%
10-15%
5-10%
1-5%
0-1%

731 **FIGURE 5**

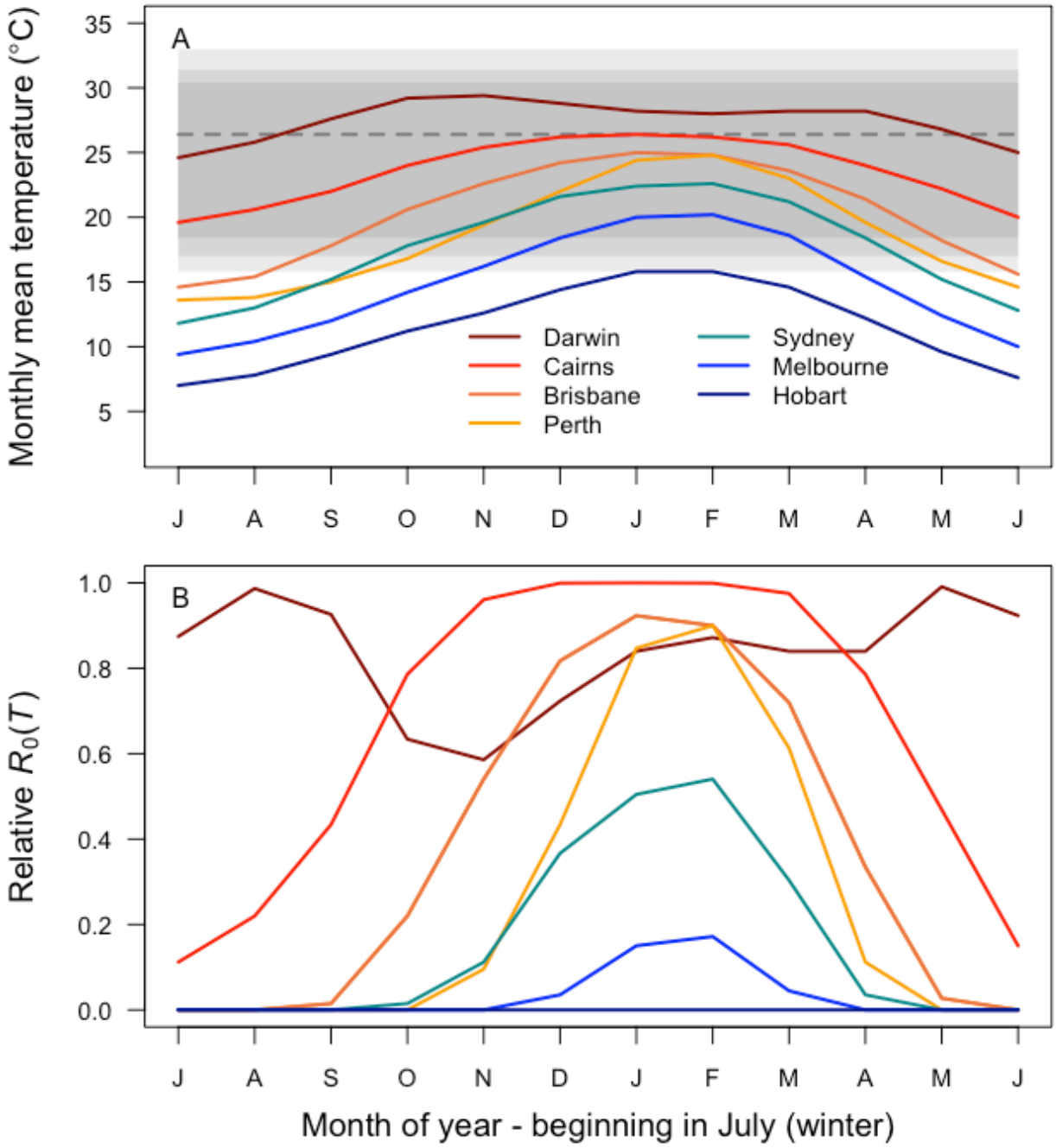

732

733

734 **FIGURE 6**

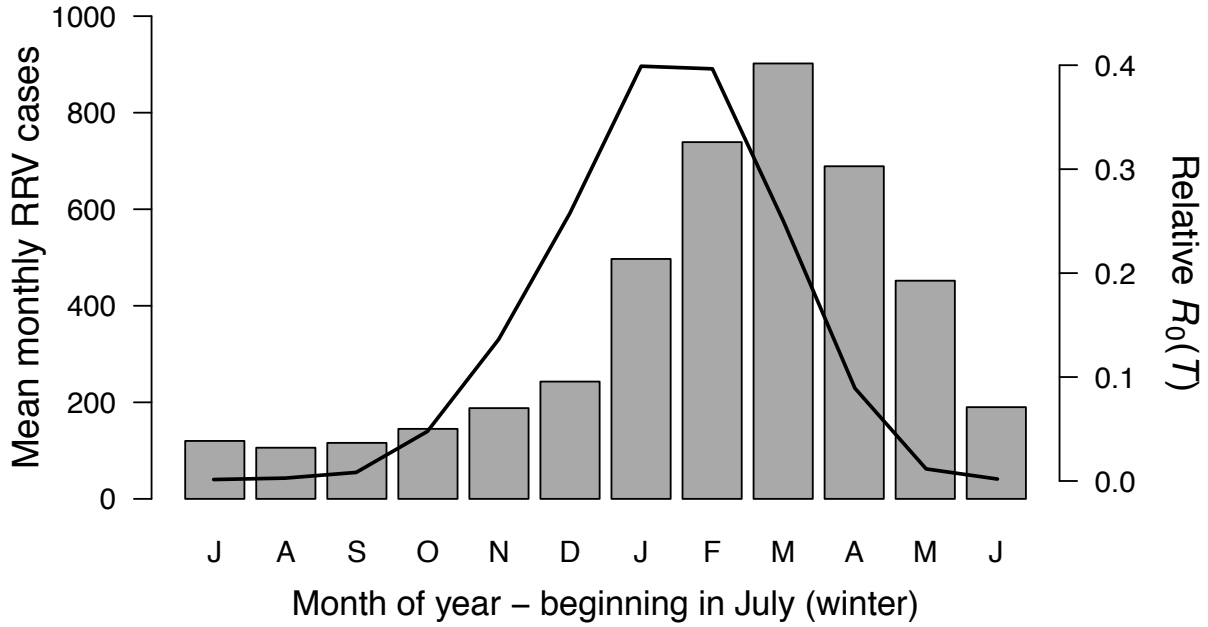

735